Title	Investigations of the radial propagation of blob-like structure in a non-confined electron cyclotron resonance heated plasma on Q-shu University Experiment with a Steady-State Spherical Tokamak
Auther(s)	Ogata, Ryota; Hanada, Kazuaki; Nishino, Nobuhiro; Liu, Haiqing; Zushi, Hideki; Ishiguro, Masaki; Ikeda, Teruaki; Nakamura, Kazuo; Fujisawa, Akihide; Idei, Hiroshi; Hasegawa, Makoto; Kawasaki, Shoji; Nakashima, Hisatoshi; Higashijima, Aki; QUEST Group,
Citation	Physics of Plasmas , 18 (9) : 092306
Issue Date	2011
DOI	10.1063/1.3640494
Self DOI	
URL	http://ir.lib.hiroshima-u.ac.jp/00033927
Right	(c) 2011 American Institute of Physics
Relation	

Investigations of the radial propagation of blob-like structure in a non-confined electron cyclotron resonance heated plasma on Q-shu University Experiment with a Steady-State Spherical Tokamak

R. Ogata,[1] K. Hanada,[2] N. Nishino,[3] H. Q. Liu,[1] H. Zushi,[2] M. Ishiguro,[1] T. Ikeda,[1] K. Nakamura,[2] A. Fujisawa,[2] H. Idei,[2] M. Hasegawa,[2] S. Kawasaki,[2] H. Nakashima,[2] A. Higashijima,[2] and QUEST Group
[1]*Interdisciplinary Graduate School of Engineering Science, Kyushu University, Kasuga, Fukuoka 816-8580, Japan*
[2]*Research Institute for Applied Mechanics, Kyushu University, Kasuga, Fukuoka 816-8580, Japan*
[3]*Department of Mechanical System Engineering, Graduate School of Engineering, Hiroshima University, Japan*

(Received 26 April 2011; accepted 12 August 2011; published online 28 September 2011)

A study of radial propagation and electric fields induced by charge separation in blob-like structures has been performed in a non-confined cylindrical electron cyclotron resonance heating plasma on Q-shu University Experiment with a Steady-State Spherical Tokamak using a fast-speed camera and a Langmuir probe. The radial propagation of the blob-like structures is found to be driven by $\mathbf{E} \times \mathbf{B}$ drift. Moreover, these blob-like structures were found to have been accelerated, and the property of the measured radial velocities agrees with the previously proposed model [C. Theiler *et al.*, Phys. Rev. Lett. **103**, 065001 (2009)]. Although the dependence of the radial velocity on the connection length of the magnetic field appeared to be different, a plausible explanation based on enhanced short-circuiting of the current path can be proposed. © *2011 American Institute of Physics*. [doi:10.1063/1.3640494]

I. INTRODUCTION

Recently, intermittent burst ejections of plasma agglomerations in the scrape-off layer (SOL) region were reported from many types of magnetic confinement devices such as NSTX,[1] Alcator C-Mod,[2] DIII-D,[3] and LHD.[4] These so-called "blobs" are a type of structure associated with turbulent fluctuations in the SOL plasma that are produced from a radially elongated structure arising from an interchange instability and that have sheared off by plasma flow from the main plasma.[5]

Radial propagation of these blobs has been extensively investigated in view of their impact on plasma confinement[6,7] as well as plasma-wall interaction (PWI).[8,9] According to one introductory model describing radial propagation velocities,[10] blobs basically propagated into the low field side riding on $\mathbf{E} \times \mathbf{B}$ drifts, where $\mathbf{E}$ and $\mathbf{B}$ are the respective electric and magnetic fields, here perpendicular to each other. The electric field can be formed initially by a self-induced charge separation due to grad $\mathbf{B}$ fields and curvature drifts and maintained at a certain value via current through the sheath at the attachment region of the metallic walls, ion polarization current,[11] and current induced by an ion-neutral friction force.[12]

The radial velocity of blobs as derived by a previously proposed model[13] can be expressed in the form

$$V_{th} = \frac{C_S}{\sqrt{R/2a_b} + (a_b/\rho_s)^2 R/L_c} \frac{\delta n}{n}, \qquad (1)$$

where $C_s = \sqrt{T_e/m_i}$ is the ion sound speed, $\rho_S = \sqrt{T_e m_i}/eB_0$ is ion Larmor radius, L_c is connection length to sheath along the magnetic field line, a_b is blob size along the electric field, R is the curvature radius (R = 1.4 m) of the toroidal magnetic field, and $\delta n/n$ describes a relative difference of a peak density from background density.[1,13] The two terms in the denominator represent a scaling factor associated with the ion polarization current (1st term) and the sheath current (2nd term). When the ion polarization current dominates, the blob velocity is approximately expressed as $V_{pol} = \sqrt{2a_b/R}C_s$. In contrast, when the sheath current dominates, the velocity is approximately $V_{she} = (\rho_s/a_b)^2 (L_c C_s/R)$.

As a conclusive comparison with theoretical models is hampered by limited accessibility for diagnostics in magnetic fusion experimental devices, instead some of detailed measurements using simulated experiments greatly contributed in clarifying the physical mechanism of blobs.[12,14] In TORPEX, experiments using electron cyclotron resonance heated (ECRH) plasmas produced by 2.45 GHz microwave were performed to simulate blobs in the SOL region of tokamaks.[14]

Radial velocities were measured to investigate the dependence on blob size and ion-neutral friction force. The main finding was that these velocities agreed with the previously proposed model based on $\mathbf{E} \times \mathbf{B}$ drift.[13] In this model, the velocity of the blobs significantly depends on the connection length L_c as obtained in Eq. (1),[13] although the dependence on L_c had not been investigated in TORPEX.

In a spherical tokamak named Q-shu University Experiment with a Steady-State Spherical Tokamak (QUEST), blob-like structures emitting intermittent bursts had been clearly observed through the combination of a Langmuir

probe and a fast-speed camera in a non-confined cylindrical plasmas generated by ECRH.[15]

In this paper, after a brief introduction to the experimental set-up in Sec. II, the results of the investigation of blob-like structure radial propagation velocities are described in Sec. III, followed by a comparison with the model given in Ref. 13 and a discussion of the results in Sec. IV. We finish with some conclusions in Sec. IV.

II. EXPERIMENTAL SET-UP

QUEST ($R_0 = 0.68$ m, $a = 0.4$ m, and $B_t = 0.25$ T at $R = 0.64$ m) is a medium-sized spherical tokamak that has the advantage of improved high beta stability compared to a conventional tokamak. It is dedicated to the study of issues related to plasma current start-up, steady-state operations, and particle recycling control.[16]

In this experiment, hydrogen plasma was produced by ECRH at 2.45 GHz in open magnetic configurations in QUEST; the field contours are depicted in Fig. 1. The injected RF power for the ECRH was approximately 10 kW. Non-confined ECRH plasmas were located around the fundamental and 2nd ECR layer at $R = 0.3$ m and $R = 0.6$ m, respectively. The 3rd and 4th ECR layers do not play an essential role in the experiment. Therefore, the outer region beyond $R = 0.6$ m to the vacuum vessel wall ($R = 1.4$ m) can be assumed to be just a propagation region for blob-like structures. Typical ECRH plasma parameters are the electron density $\sim 1\text{–}5 \times 10^{16}$ m^{-3}, the electron temperature 4–12 eV, and the plasma potential 10–20 V.

A vertical magnetic field B_z of magnitude 6.4–24 mT was superimposed on a 39 mT toroidal field B_T at $R = 0.64$ m. B_z is held constant for all radial directions on the mid-plane ($Z = 0$ m) of the vacuum vessel. In contrast, B_T is inversely proportional to the radial distance. QUEST has two flat divertor plates at $Z = \pm 1$ m from the mid-plane, as marked in Fig. 1. The dependence of the radial propagation velocity on L_c is investigated by changing B_z, and the results were compared with those obtained by a model presented in Ref. 13. L_c is estimated from the connected length along the magnetic field between the two flat divertor plates through the sheath, and it can be obtained from Eq. (2) if the plasma current is neglected. Here B_R and B_Z are the radial and vertical magnetic fields, respectively, R, Z, θ the major radius, vertical, and rotation directions, respectively, $dl = \sqrt{d_R^2 + d_Z^2 + (Rd_\theta)^2}$.

$$L_c = \int_{-L}^{L} \sqrt{1 + \frac{B_{R(R,Z,\theta)}^2}{B_{Z(R,Z,\theta)}^2} + \frac{B_{T(R,Z,\theta)}^2}{B_{Z(R,Z,\theta)}^2}}\, dz. \quad (2)$$

Here, L represents the vertical distance of the flat divertor plate from the mid-plane. The blob-like structures were measured with both a fast-speed camera and a Langmuir probe. Fig. 2 shows a schematic view of the location of the probe system and camera. The camera was located at a toroidal angle of 92.5° away from the probe system, and its wide viewing angular range of 72° enables monitoring of what is happening at the probe head (R is less than 0.9 m approximately). Typically, the fast-speed CCD camera is set at 50 μs per frame recording 288×240 pixel images in each frame. For measuring, two types of probe head with six pins were affixed. For the first type, sketched on the left side of Fig. 3, opposing pins are separated by distance $l_z = 5$ mm and pairs of pins with a radial-separation of $l_R = 14$ mm. The second type is shown on the right side of Fig. 3. Measurements taken in combination with the fast speed camera were only obtained by using the second type. Pins on both probe heads are identified by letters A–F. The ion saturation current (A-pin(I_{sat1}) and B-pin(I_{sat2})), the positive bias (C-pin(V_{+2}) and D-pin(V_{+1})), and the floating potential (E-pin(V_{f1}) and F-pin(V_{f2})) can be measured with a sampling rate of 1 MHz. The ion saturation current I_{sat} is proportional to the product of the density and the sound speed of plasma, $nT^{0.5}$. Accordingly, by neglecting the time variation of the temperature, the ion saturation current can be regarded as a density.

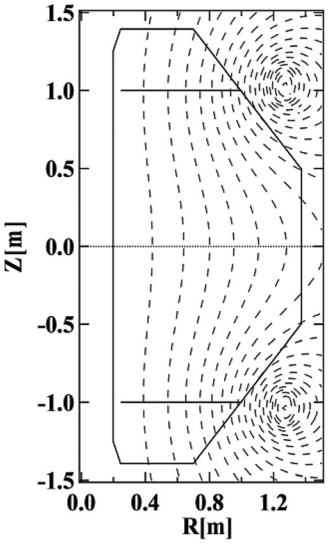

FIG. 1. Cross-sectional side view of QUEST is shown. Dash lines show a typical magnetic flux surface in an open magnetic configuration employed in the experiments. Two solid horizontal lines represent the position of flat divertor plates.

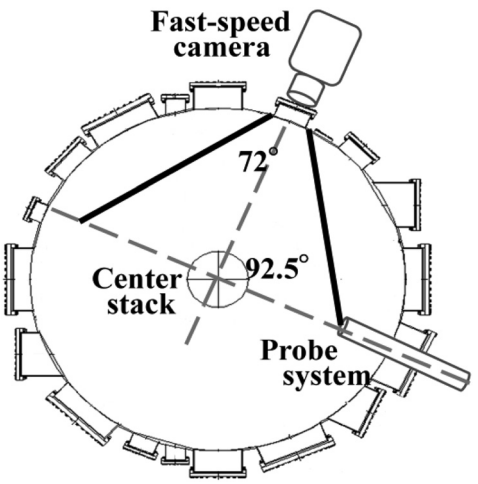

FIG. 2. A schematic view through the mid-plane ($Z = 0$ m) showing the location in QUEST of the probe system and the fast-speed camera.

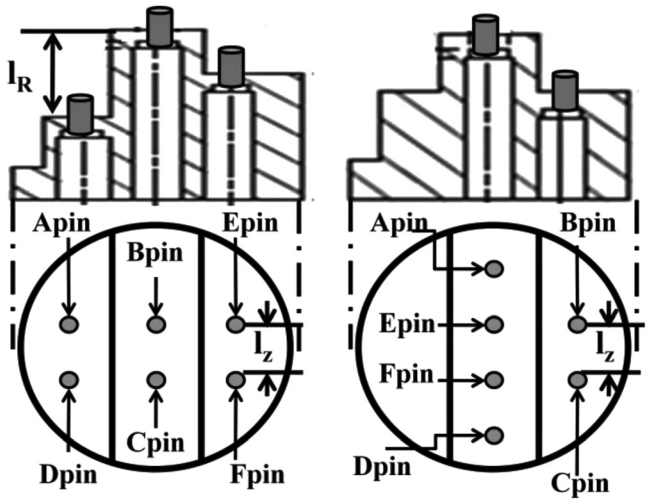

FIG. 3. Side and front views of two types of probe head. Each probe pin in the figure is identified by its label.

The radial velocity V_b of blob-like structures is directly measured with the first type of probe as follows. The time evolution of I_{sat} at two different radial positions (A-pin and B-pin) separated by distance $l_z = 14$ mm was measured, and the time lag (Δt) of the measured signals was obtained from cross-correlations using the reconstruction method of the wavelet transform of the signal.[17] Finally, the radial velocities of blob-like structures can be estimated from $V_r = l_R/\Delta t$. The velocity of intense radially propagating emissions from blob-like structures, V_{image}, were investigated by analyzing emission intensities I_{hv} derived from visible images measured with the fast-speed camera. The visible images are mainly attributable to Hα emissions which are radiated through collisions between hydrogen atoms and electrons. By assuming that the density n_0 of hydrogen atoms is uniform in the vacuum vessel, the visible image can directly reflect the electron density distribution,[18,19] and for this reason the estimated V_{image} has sometimes been regarded as the radial velocity of blobs in the previous research.[1,2] However, this aspect should at least be confirmed by performing experiments.

Some intense emissions have appeared on images when blob-like structures have been generated and propagate. These emissions as seen in every frame move outwards the low field side. Therefore, cross-correlation analysis of the radial $I_{hv}(R)$ profile ($Z = 0$ m) was performed every 50 μs using Eq. (3).

$$C_v(m) = \sum_{k=1}^{N} I_{hv}(k)_n \cdot I_{hv}(k+m)_{n+1}. \tag{3}$$

Here C_v is the cross-correlation value, N is the pixel number in the radial direction, n is the frame number, and $k = 1, 2 \cdots N$. The propagation distance, Δd_p, is obtained from the highest amplitude value of the cross-correlation such as $\Delta d_p = m_p \times 0.007$ [m]. Value of 0.007 m indicates each pixel size of the fast camera, and V_{image} can be estimated as $V_{image} = \Delta d_p/5 \times 10^{-5}$.

III. ANALYSIS AND EXPERIMENTAL RESULTS

To begin, the radial velocity of the blob-like structures was compared with the $\mathbf{E} \times \mathbf{B}$ drift velocity. We shall briefly describe how the electric field is estimated from the probe signals. The axial component of the electric field E_z was measured from the potential difference between the E- and F-pins using $E_Z = (V_{f1} - V_{f2})/l_z$. A time evolution of E_z is shown in Fig. 4(a). As a blob approaches the probe pins, the E_z signal rises positively indicating that an E_z component exists inside the blob-like structure as predicted by the theory introduced in Sec. II. However, before the blob reaches the probe pins, E_z has already been observed. We use E_z weighted by I_{sat} as indicated in Eq. (4).

$$\langle E \rangle_b = \frac{\int I_{sat}(t) E_z(t) dt}{\int I_{sat}(t) dt}. \tag{4}$$

The main $\langle E \rangle_b$ contribution comes from the high density region of blob-like structures. Most values are zero in I_{sat}, except when the blob-like structure passes the probe. However, the E_z values fluctuate because of the presence of background plasma that generates positive spikes as the blob-like structure passes, as seen in Fig. 4(a). Therefore, most of background signal can be cancelled by weighting I_{sat} as demonstrated in Fig. 4(b). The $\mathbf{E} \times \mathbf{B}$ drift velocity of the blob-like structure, as it passes the probe, can be estimated at about $V_{E\times B} = \langle E \rangle_b / B_T \sim 40(V/m)/27(mT) = 1.5$ km/s by integrating the area under the curve, where the background vanishes sufficiently, as obtained in Fig. 4(c).

Fig. 4(d) shows the two simultaneously measured signals of the ion saturation currents. The time lag Δt, clearly observed in the figure, was 10 μs when the cross-correlation was performed. V_b, as the time the blob-like structure passes the probe, can be estimated to be $\sim$1.4 km/s, which agrees reasonably-well with the $\mathbf{E} \times \mathbf{B}$ drift velocity.

A comparison of $V_{E\times B}$ and V_b is shown in Fig. 5. The clustering of results near the diagonal clearly indicates that the radial velocity of blob-like structure is almost equivalent to the measured $\mathbf{E} \times \mathbf{B}$ drift velocity: Therefore the radial propagation of these structures has been driven by $\mathbf{E} \times \mathbf{B}$ drift. Hereafter, we regard the measured $\mathbf{E} \times \mathbf{B}$ drift velocities as radial velocities of the blob-like structures.

The top panel of Fig. 6 shows the radial dependence of the $\mathbf{E} \times \mathbf{B}$ drift velocities of blob-like structures as measured with the second probe head and V_{image} as imaged with the fast-speed camera and compared with the model of Ref. 13. The middle panel graphs shows the average values (with error bars) of the plasma parameters associated with blob-like structure formation used in the evaluation of velocities. Using the camera images, values of blob-like structure size a_b along the electric field were estimated to be approximately 0.08 m. The value of a_b is defined as the average of the FWHM of the vertical profiles for the light-intensities from blob-like structures. The estimation of a_b strongly depends on the resolution of the camera, and moreover the images represent not the density, but just the visible light distribution. Therefore, a measurement was performed for checking the accuracy of the estimation of blob sizes using the camera image. We could estimate radial sizes by both the probe and

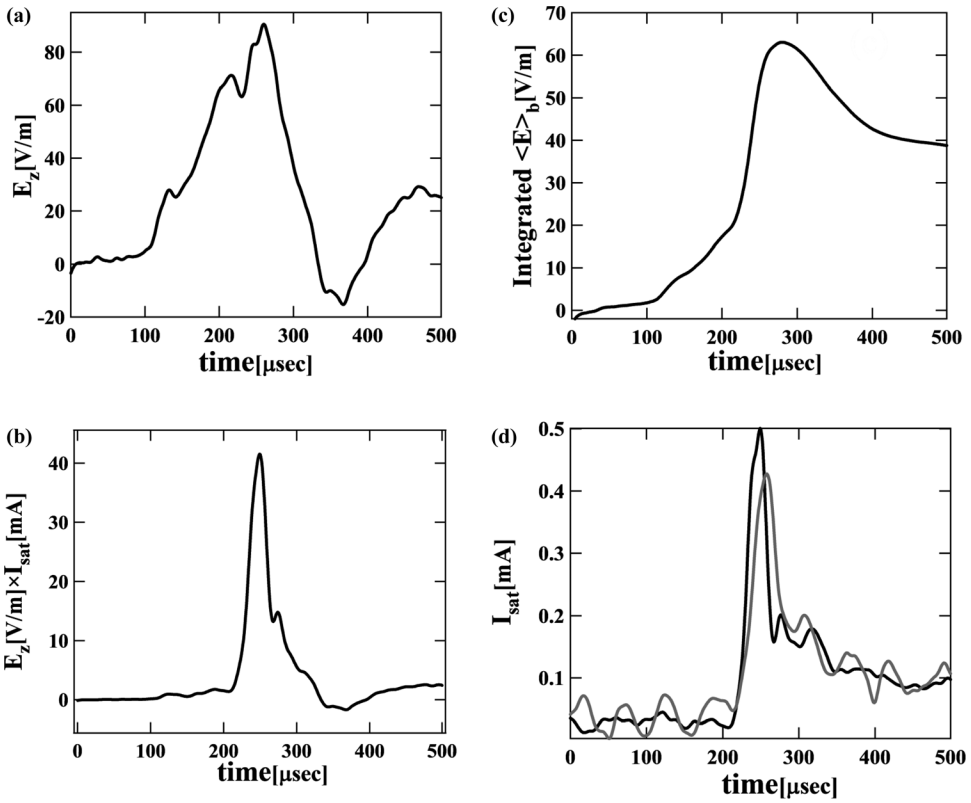

FIG. 4. Typical time evolutions of (a) E_z, (b) product E_z with I_{sat}, (c) the normalized integrated value, $\langle E \rangle_b$, and (d) I_{sat} around a passing blob. The black and gray lines in panel (d) correspond to I_{sat2} and I_{sat1}, respectively. The probe was located at $R = 0.95$ m, where $B_z \sim 16$ mT and $B_T \sim 27$ mT were applied over the mid-plane region.

the camera in the case of $L_c = 4.1$ m, and we could compare each other. A radial blob-like structure size could be measured from probe measurements ($\sim$0.065 m) and camera images ($\sim$0.08 m), independently. Thus, the radial size measured from images differs by roughly +20% compared with the probe measurements. Vertical size of blob-like structures as determined from the camera images have been corrected by 20%.

The values of $V_{E\times B}$ and V_{image} were compared at $R \sim 0.65$ m and $R \sim 0.85$ m. The value of V_{image} near the second ECR layer ($R = 0.7$ m) was approximately 0.9 km/s, while at $R = 0.8$ m, V_{image} was higher at approximately 1.2 km/s; $V_{E\times B}$ was approximately 1.0 km/s at $R = 0.65$ m and approximately 1.3 km/s at $R = 0.75$ m. The absolute values

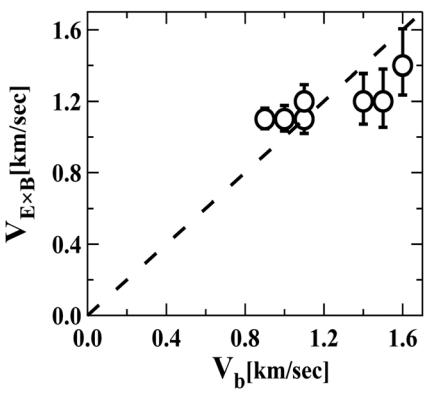

FIG. 5. Results of the simultaneous measurement of $V_{E\times B}$ and V_b by the probe at $R = 0.8$ m. The black-dashed line identifies the equivalence of the velocities.

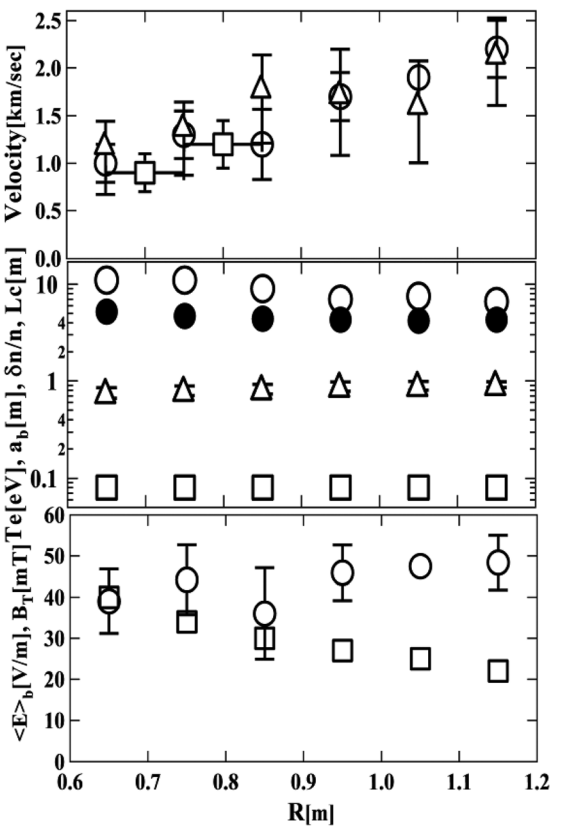

FIG. 6. Top: the radial profiles of the $V_{E\times B}$ (circles) estimated by radial scanning measurement, the V_{image} (squares), and V_{th} (triangles). Middle: electron temperature (circles), $\delta n/n$ (triangles), blob size (squares), and connection length (solid-circles). Bottom: the radial profiles of $\langle E \rangle_b$ (circles) and B_T (squares). The $B_z \sim 16$ mT was applied on the mid-plane region.

of $\mathbf{E}\times\mathbf{B}$ drift velocities agree with those of V_{image}, so that V_{image} can be also regarded as giving actual blob radial velocities. Moreover, it is clear that $V_{E\times B}$ and V_{image} tend to increase in going to the low field side.[8] This implies that blob-like structures have been accelerated. The region beyond $R=0.85$ m is out of range of the fast-speed camera view. The value of $\langle E\rangle_b$ was constant along the radial direction. In contrast, B_T is inversely proportional with major radius as seen in the bottom panel of Fig. 6.

In considering acceleration mechanisms, gradients of the magnetic pressure arising from the toroidal field and the plasma pressure were estimated. The magnetic pressure gradient, $\nabla\left(B_T^2/2\mu_0\right)$, ranged from ~2000 Pa/m at $R=0.65$ m to ~500 Pa/m at $R=1.15$ m. In contrast, the plasma pressure gradient, $\nabla(kn_eT_e)$, ranged from ~0.5 Pa/m at $R=0.65$ m to ~0.05 Pa/m at $R=1.15$ m, where μ_0 is the vacuum permittivity, k the Boltzmann constant, T_e the electron temperature, and n_e the electron density. The values of T_e and n_e were obtained from probe measurements. The plasma pressure was significantly less by a thousandth compared with the magnetic pressure, and plasma beta is as low as $\beta\sim10^{-4}$. Therefore, the effect of plasma pressure can be neglected, leaving the effects including the theoretical model shown in Eq. (1) to dominate blob acceleration in the toroidal field and the radial propagation velocity having positive dependence on the radial position.

Moreover, V_{th} was in full accord both in scale and trend with the measured velocity at each radial position. In considering what the most dominant effect is, we calculate both V_{she} and V_{pol} based on the experimental observations, and the result is shown in Fig. 7. This indicates that the electric field of blob-like structures can almost be limited by the sheath current, because radial velocity related to a dominant effect is the slowest. In fact, the values of V_{pol} are approximately 11 km/s for all L_c conditions, and this implies that the polarization current is significantly smaller than the sheath current and the sheath current is dominant in the experiments. In the scaling law presented in Ref. 13, effects of ion-neutral collisions were also considered. The estimated radial velocities related to ion-neutral collision corresponds to approximately 100 km/s and, it found that in QUEST, ion-neutral collisions have no effect compared with the other processes associated with the ion polarization current and sheath current. Therefore, the effect of ion-neutral collisions can also be neglected. These results indicate that the experiments in QUEST were operating in the electrostatic regime for blob propagation[1,20] and that this observation does not contradict the fact that blob-like structure radial velocities are predominantly driven by $E\times B$ drifts.

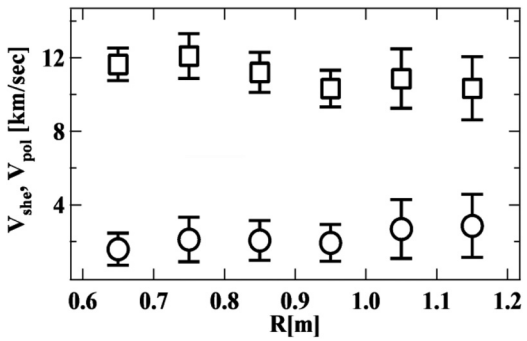

FIG. 7. Radial profile of V_{she} (circles) and V_{pol} (squares) derived from the experimental observation shown in Fig. 6.

To investigate the accuracy of the theoretical prediction, the experiments varying L_c were performed. Blob-like structures could be modified by varying the ratio B_Z/B_T.[21,22] Therefore, L_c can be varied by varying this ratio. The top panel of Fig. 8 shows V_{th}, $V_{E\times B}$ ($R=0.9$ m) and V_{image} ($R=0.8$ m) as functions of L_c: The bottom panel gives the average values and error bars of plasma parameters for blob-like structures used in the evaluation of theoretical velocities in investigating the L_c dependence. There was a change also in T_e and $\delta n/n$ when the connection length changed. Values of $T_e=10.5$, 6.5, 5.5 eV and $\delta\ n/n=0.79$, 0.89, 0.95 (for $L_c=9.3$, 4.1, 3.2 m, respectively) were obtained with the probe signals.

The calculated result of V_{th} shows that V_{th} increases with L_c. In contrast, the measured velocities $V_{E\times B}$ and V_{image} decrease with increasing L_c. According to the model of Ref. 13, the electric field of blob-like structures must be strong when the elongated connection length prevents short-circuiting at the sheath region, and as the result, the $\mathbf{E}\times\mathbf{B}$ drift velocity must increase. However, the measured $\langle E\rangle_b$ decays with increasing L_c, and this tendency does not agree with the model. Some reasons of this disagreement will be discussed in Sec. IV.

IV. DISCUSSION

Blob-like structures observed in QUEST are accelerated when traversing to the low field side beyond $R=0.6$ m. However, in DIII-D,[3] blobs propagate radially with $\mathbf{E}\times\mathbf{B}$ drift velocities while decelerating from ~2.6 km/s near the last closed flux surface (LCFS) to ~0.33 km/s near the vacuum

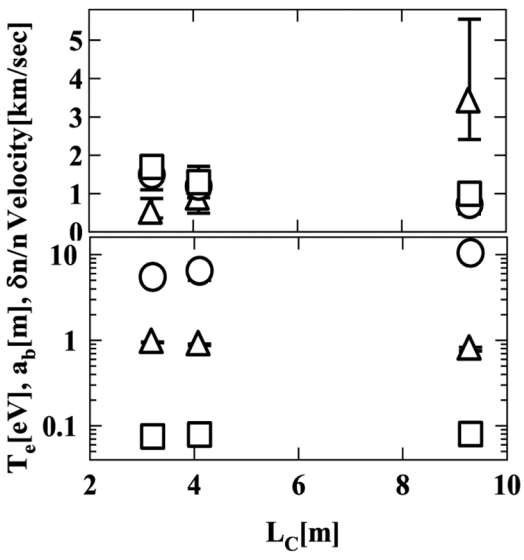

FIG. 8. Top: V_{th}, $V_{E\times B}$ ($R=0.9$ m) and V_{image} ($R=0.8$ m) were plotted as function of L_c. The circle-, square- and triangle-marker show the $V_{E\times B}$, V_{image}, and V_{th}, respectively. Bottom: average value of plasma parameter of the blob-like structure. The circle-, square-, and triangle-marker show T_e, a, and $\delta n/n$, respectively.

vessel. Such behavior was also reported by Alcator C-Mod (Ref. 2) and HL-2A tokamak.[23] The propagating region of the blobs in those experiments was too narrow at approximately 0.05 m and the variation of major radius significantly small that any effects would be hard-pressed to accelerate blobs. Even in those experiments, radial velocities were consistent with $\mathbf{E}\times\mathbf{B}$ drift velocities. While in QUEST, the observed propagating distance of blob-like structures is significantly wide at approximately 0.7 m, and the major radius was varying in the propagating region. Thus, the dependence on the major radius including in the theory clearly appeared as acceleration of blob-like structures.

The observed dependence on L_c seems to disagree with the model of Ref. 13. An experiment had already been performed to provide a comparative study with theoretical models in TORPEX, and results agreed with the model expectations.[13] However, the applied B_z/B_T rate of ~0.02 is rather small; in addition, the connection length was fixed by a metal limiter.[13] In our experiment, the applied B_z/B_T rate was 0.16–0.62. It is not possible to compare simply our result with the TORPEX experimental result, because the mechanism of charge separation strongly depends on the magnetic field configuration and strength. When a large superimposed vertical magnetic field was applied, the short-circuiting currents flow only within the sheath region as predicted by our proposed model, the value of L_c being determined by the ratio of B_Z/B_T. When small values of B_Z are applied, as performed in QUEST, the pitch of the magnetic field lines becomes narrow, and a significant connection current between the pitch of the blob-like structure may flow, as illustrated in Fig. 9. It is thought that this situation is produced by an inverse electric field in the inside of the blob-like structure between the pitch of the blob-like structures as shown in the illustration of Fig. 9.

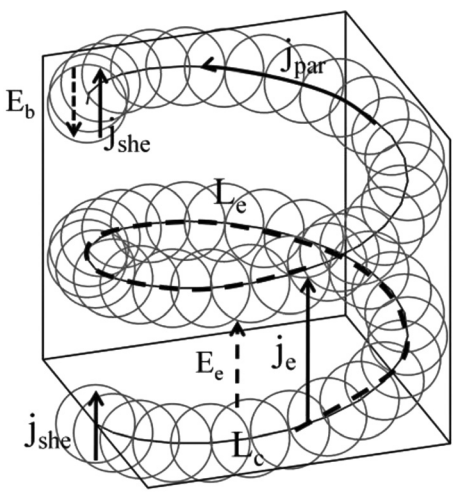

FIG. 9. Schematic of a blob-like structure in QUEST. In the previously proposed model, a return current exists only in the sheath region (j_{she}). When the pitch of a blob-like structure is shortened, the return current may flow between the pitch (j_e). The black solid-line traces out the connection length L_c, and the black dashed-line the effective connection length L_e. j_{par} signifies the parallel current, j_{she} the return current in the sheath region, and j_e the short-circuiting current. The E_b and E_e show the direction of the electric field inducted in internal blob-like structure and between the pitch of the blob-like structure, respectively.

Fig. 10 shows the waveform of the electric field (a), the waveform of the ion saturation current (b), and the fast-speed camera image (c) when the probe had taken measurements between the pitch of blob-like structures. The fast-speed camera image was observed very clearly under such conditions. The electric field that had been measured corresponded to a negative spike, which was observed a lot in plasmas applied the small ratios of B_Z/B_T. Simultaneously, a significant increment of ion saturation current also was observed. The dense plasma existing between the pitch regions of the blob-like structures can drive the enhanced canceling current, j_e, ascribed to the curvature and grad-B drift motion as shown in Fig. 9. These observations suggest that short-circuiting currents exist between the pitch of the blob-like structures. The short-circuiting current proposed here has been clarified in the theory as shown in the difference between δn and n. Background plasmas nestled between the two blobs naturally drives a certain amount of current because of their charge separation, and this leads to

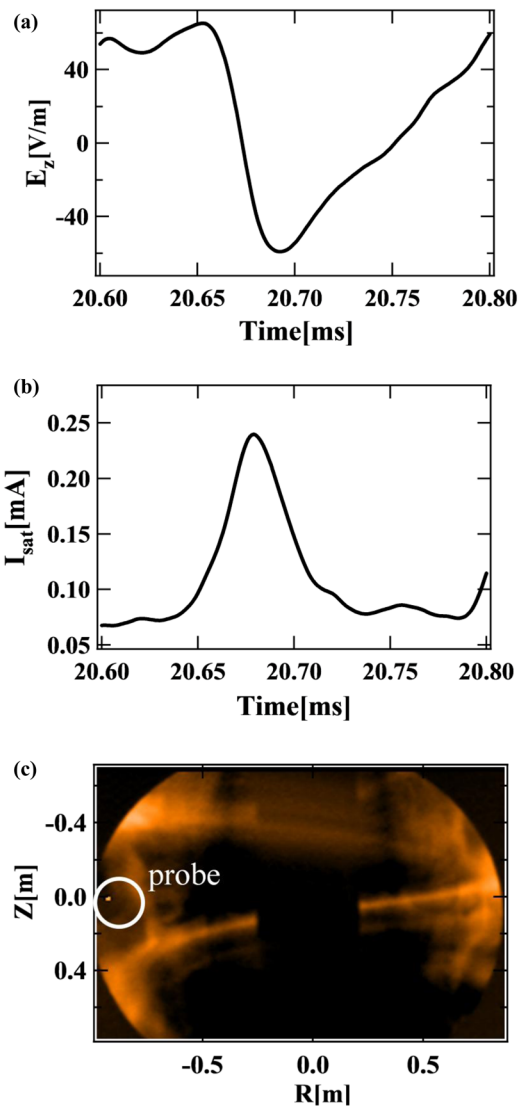

FIG. 10. (Color online) The waveform of electric field (a), the waveform of ion saturation current (b), and the fast-speed camera image (c) when the probe measured between the pitch of blob-like structures. The fast-speed image was obtained at 20.7 ms.

reduction of return current in blobs. Therefore, the required amount of return current is proportional to $\delta n/n$ in the theory. In experimental views, δn has been derived from a background plasma density at the time just before and after a targeted blob has passed; however, our observation showed that the background density derived from the above-described way is significantly different from an original value of background density being supposed to use in the estimation of δn.

As a result, the effective connection length shortens, and the observed radial motion was slower. This may qualitatively explain the disagreement in the L_c dependence of the radial velocity in QUEST. Moreover, the shortened connection length may appear in the SOL region of a tokamak and may diminish propagation velocities. Although we would like to consider some reasons why the enhanced background density is happened in the longest Lc case, we could not get any clear answers. A detailed study is left for future work.

V. CONCLUSION

An investigation of the radial propagation mechanism for blob-like structures was performed in a non-confined ECRH plasma on QUEST. The $\mathbf{E} \times \mathbf{B}$ drift velocity was found to agree reasonably well with radial propagation velocities that had been measured simultaneously with a probe and a camera. Analysis indicated that blob-like structures were accelerated along with the radial propagation and the positive dependence of the radial propagation velocity on the radial position in the field was in full accord both in scale and trend with the measured velocity at each radial position. Magnetic connection length dependencies in the $\mathbf{E} \times \mathbf{B}$ drift velocities do not seem to be explained by the model based on induced electric fields from charge separation and current paths. Dense plasmas existing between the pitch regions of the blob-like structures were observed in the longest connection length case, and the related enhanced short-circuiting currents make the radial propagation slower.

ACKNOWLEDGMENTS

This work was performed with the support from and under the auspices of the NIFS Collaboration Research Program (NIFS08KUTR024).

[1]J. R. Myra, D. A. D'Ippolito, D. P. Stotler, S. J. Zweben, B. P. LeBlanc, J. E. Menard, R. J. Maqueda, and J. Boedo, Phys. Plasma **13**, 92509 (2006).
[2]O. Grulke, J. T. Terry, B. LaBmbard, and S. J. Zweben, Phys. Plasma **13**, 12306 (2006).
[3]J. A. Boedo, D. L. Rudakov, R. A. Moyer, G. R. McKee, R. J. Colchin, M. J. Schaffer, P. G. Stangeby, W. P. West, S. L. Allen, T. E. Evans, R. J. Fonck, E. M. Hollmann, S. Krasheninnkov, A. W. Leonard, W. Nevins, M. A. Mahdavi, G. D. Porter, G. R. Tynan, D. G. Whyte, and X. Xu, Phys. Plasma **5**, 1670 (2003).
[4]N. Ohno, S. Masuzaki, H. Miyoshi, S. Takamura, V. P. Budaev, T. Morisaki, N. Ohyabu, and A. Komori, Controlled Plasma Phys. **46**, 692 (2006).
[5]O. E. Garcia, J. Horacek, R. A. Pitts, A. H. Nielsen, W. Fundamenski, J. P. Graves, V. Naulin, and J. J. Rasmussen, Plasma Phys. Controlled Fusion **48**, L1 (2006).
[6]G. S. Xu, V. Naulin, W. Fudamenski, C. Hidaigo, J. A. Alonso, C. Silva, B. Goncalves, A. H. Nielsen, J. J. Rasmussen, S. I. Krasheninnikov, B. N. Wan, M. Stamp, and JET EFDT Contributors, Nucl. Fusion **49**, 92002 (2009).
[7]J. Horacek, J. Adamek, H. W. Mueller, J. Seidl, A. H. Niesen, V. Rohde, F. Mehmann, C. Ionita, E. Havlickva, and ASDEX Upgrade Team, Nucl. Fusion **50**, 105001 (2010).
[8]H. Q. Liu, K. Hanada, N. Nishino, R. Ogata, M. Ishiguro, H. Zushi, K. Nakamura, A. Fujisawa, M. Sakamoto, H. Idei, M. Hasegawa, S. Kawasaki, H. Nakashima, A. Higashijima, and QUEST Group, J. Nucl. Mater. (to be published).
[9]I. Nanobashvili, J. P. Gunn, and P. Devynck, J. Nucl. Mater. **363–365**, 622 (2007).
[10]S. I. Krasheninnikov, Phys. Lett. **A283**, 368 (2001).
[11]O. E. Garcia, N. H. Bian, V. Naulin, A. H. Nielsen, J. J. Rasmussen, Phys. Plasma **12**, 90701 (2005).
[12]N. Katz, J. Egedal, W. Fox, A. Le, and M. Porkolab, Phys. Rev. Lett. **101**, 15003 (2008).
[13]C. Theiler, I. Furno, P. Ricci, A. Fasoli, B. Labit, S. H. Muller, and G. Plyushchev, Phys. Rev. Lett. **103**, 065001 (2009).
[14]S. H. Muller, C. Theiler, A. Fasoli, I. Furno, B. Labit, G. R. Tynan, M. Xu, Z. Yan, and I. H. Yu, Plasma Phys. Controlled Fusion **51**, 55020 (2009).
[15]H. Q. Liu, K. Hanada, N. Nishino, R. Ogata, M. Ishiguro, H. Zushi, K. Nakamura, A. Fujisawa, M. Sakamoto, H. Idei, M. Hasegawa, S. Kawasaki, H. Nakashima, A. Higashijima, and QUEST Group, J. Plasma Fusion Res. **5**, S2077 (2010).
[16]K. Hanada, K. Sato, H. Zushi, K. Nakamura, M. Sakamoto, H. Idei, M. Hasegawa, Y. Takase, O. Mitarai, T. Maekawa, Y. Kishimoto, M. Ishiguro, T. Yoshinaga, H. Igami, N. Nishino, H. Honma, S. Kawasaki, H. Nakashima, A. Higashijima, Y. Higashizono, A. Ando, N. Asakura, A. Ejiri, Y. Hirooka, A. Ishida, A. Komori, M. Matsukawa, O. Motojima, Y. Ogawa, N. Ohno, Y. Ono, M. Peng, S. Sudo, H. Yamada, N. Yoshida, and Z. Yoshida, J. Plasma Fusion Res. **5**, S1007 (2010).
[17]N. Ohno, V. P. Budaev, K. Furuta, H. Miyoshi, and S. Takamura, Controlled Plasma Phys. **44**, 222 (2004).
[18]S. J. Zweben, R. J. Maqueda, D. P. Stoter, A. Keesee, J. Boedo, C. E. Bush, S. M. Kaye, B. LeBlanc, J. L. Lowrance, V. J. Mastrocola, R. Maingi, N. Nishino, G. Renda, D. W. Swain, J. B. Wilgen, and NSTX Team, Nucl. Fusion **44**, 134 (2004).
[19]S. J. Zweben, D. P. Stotler, J. L. Terry, B. LaBombard, M. Greenwald, M. Muterspaugh, C. S. Pitcher, K. Hallatschek, R. J. Maqueda, B. Rogers, J. L. Lowrance, V. J. Mastrocola, G. F. Renda, and Alcator C-Mod Group, Phys. Plasma **9**, 1981 (2002).
[20]S. I. Krasheninnikov, D. A. D'ippolito, and J. R. Myra, Phys. Plasma **74** 679 (2008).
[21]H. Zushi, N. Nishino, K. Hanada, H. Honma, H. Q. Liu, Y. Higashizono, M. Sakamoto, S. Tashima, T. Ryoukai, and QUEST Group, J. Nucl. Mater. (to be published).
[22]H. Q. Liu, K. Hanada, N. Nishino, R. Ogata, M. Ishiguro, H. Zushi, K. Nakamura, A. Fujisawa, M. Sakamoto, H. Idei, M. Hasegawa, S. Kawasaki, H. Nakashima, A. Higashijima, and QUEST Group, J. Plasma Fusion Res. Series, **9**, 33 (2010).
[23]J. Cheng, L. W. Yan, W. Y. Hong, K. J. Zhao, T. Lan, J. Qian, A. D. Liu, H. L. Zhao, Yi Liu, Q. W. Yang, J. Q. Dong, X. R. Duan, and Y. Liu, Plasma Phys. Controlled Fusion **52**, 55003 (2010).